ISSN (Online) 2456-1290

International Journal of Engineering Research in Mechanical and Civil Engineering (IJERMCE)

Volume 12 Issue 12 December 2025

PLIF Visualisation and Qualitative Investigation on Plume Structure in Natural Convection

[1] Syam Joy, [2] Franklin R John*, [3] Joshy P J, [4] Baburaj A Puthenveettil

[1][2][3] Division of Mechanical Engineering, School of Engineering, CUSAT
[4] Department of Applied Mechanics & Biomedical Engineering, IIT Madras, India
Email: [1] samjoy009@gmail.com, [2] frankcusat@gmail.com, [3] pjjoshy1969@gmail.com, [4] apbraj@gmail.com

Abstract*— Planar Laser Induced Fluorescence visualisation (PLIF) of plume structures erupting from the species boundary layer formed over a semi-permeable membrane is conducted by having an unstable density difference across the semi-permeable membrane. The experiments were conducted at Prandtl number, Pr ~ 610, and over a range of Rayleigh number 3.1 ×1011 < RaH < 6.12 × 1010. The near membrane structures consist of line plumes erupting from the species boundary layer due to unstable density difference of having high concentration fluid (NaCl) in the top tank and low concentration fluid (NH4Cl) in the bottom tank. The pore size of the membrane allows advection across the membrane. The evolution of plumes from the species boundary layer was studied at different concentration differences, 2 < ΔC < 10. Three phases were observed in the evolution, viz, Pouring dominant phase, Transition phase and fully developed plume field. The planform of a fully developed plume structure consists of three zones: plume free region due to impingement of circulatory through flow across the membrane, aligned plume region where the plumes rising from the boundary layer are aligned in the direction of large-scale flow and instability driven plume region where the evolution of plumes isn't affected by shear. At constant RaH, the mean plume spacing in the shear-affected zone was found to be smaller than the instability-driven plume region.

Index Terms*— Convection Across Semipermeable Membrane, Plume Structures, Advection, Circulation, Rayleigh Number, Prandtl Number

I. INTRODUCTION

Convection across a semipermeable membrane is a type of natural convection process due to an unstable density difference across the membrane. In such convection species boundary layer is formed over the semi-permeable membrane; this is analogous to the formation of a thermal boundary layer in Rayleigh-Benard convection. At sufficiently high Rayleigh number, these boundary layer develops instability and erupt to form plume structures. In convection from a high-temperature bottom plate to a fluid, these plumes carry the majority of heat into the bulk, whereas in convection across a semi-permeable membrane, plumes carry the majority of flux into the bulk.

Natural convections are generally classified into direct and indirect convections; In direct natural convections density gradient is directly imposed, whereas in indirect natural convections boundary layer over a horizontal surface is developed indirectly, as in the studies of Schlichiting and Gersten (2003). In the present study, the species boundary layer over the semi-permeable membrane is inherently unstable because of high-density fluid in the top tank and a low-density fluid in the bottom tank. The onset of convection is marked by the eruptions of plumes from the boundary layer when the buoyancy force overcomes the diffusive effects Sparrow and Huser (1969). In the present study, we employ a planar laser-induced fluorescence visualisation technique to capture the sheet plumes erupting from the boundary layer; these sheet plumes appear as bright lines with complex dynamics in the horizontal planar laser sheet when viewed from above. Visualisation of plume structures emerging from a boundary layer has historically relied on a variety of experimental techniques, each of which identifies plumes based on an implicit detection criterion. In the present study, we employ planar laser-induced fluorescence (PLIF) to capture the plume structures rising from the species boundary layer. This approach detects plumes as regions of enhanced fluorescence, corresponding to zones with locally higher concentrations of the fluorescent dye.

Much of the current understanding of line plumes in turbulent convection is derived from earlier visualisation experiments that used different physical signatures to identify plume regions. Electrochemical visualisation methods, for example, typically reveal plumes as darker zones where the concentration of a dark dye exceeds a detectable threshold (Sparrow and Husar 1969; Adrian, Ferreira and Boberg 1986; Theerthan and Arakeri 1998). In contrast, laser-induced fluorescence techniques detect plumes as brighter, strongly fluorescing regions because of the elevated dye concentration along the plume core (Puthenveettil 2004; Puthenveettil, Ananthakrishna and Arakeri 2005; Ramareddy and Puthenveettil 2011). Other diagnostic approaches rely on different plume attributes. In flows seeded with temperature-sensitive liquid crystals, plumes appear in regions where the temperature is locally higher, allowing thermal visualisation of the plume field (Zhou and Xia 2010). Shadowgraphy, which responds to refractive-index gradients, identifies plumes as regions of relatively lower density (Bosbach, Weiss and Ahlers 2012). Similarly, in visualisations using smoke particles illuminated by a laser sheet, plumes manifest

ISSN (Online) 2456-1290

International Journal of Engineering Research in Mechanical and Civil Engineering (IJERMCE)

Volume 12 Issue 12 December 2025

as regions where particle concentration decreases due to plume-induced entrainment and displacement (Puthenveettil *et. al* 2011; Gunasegarane and Puthenveettil 2014). Collectively, these diverse techniques—ranging from electrochemical and dye-based visualisations to shadowgraphy, TSLC imaging, and particle-scattering methods—provide a consistent framework for detecting and characterising plume structures. Pera and Gebhart (1973) observed that the line plumes of low-density fluids are formed from gravitational instability. After erupting from the boundary layer, they rise as sheet plumes exhibiting later motion and merging. For a very small finite height, measured vertically above the boundary layer, these plumes have a finite thickness beyond which they diffuse to form a mushroom-like structure, dissipating flux into the bulk. In the studies of Theerthan and Arakeri (1998), Baburaj and Arakeri (2008), Baburaj *et.al* (2011), Gunasegarane and Baburaj (2014), Baburaj and Arakeri (2005), Shevkar *et.al* (2002), Ramareddy *et.al* (2020), and Joshy *et.al* (2023), plume structures were quantified based on the total length (L_p), mean plume spacing (λ), mean plume thickness (t_p) and plume area ratio (A_p/A). The *Ra* and *Pr* dependence on the mean properties of plume structures was empirically obtained by Zhou and Xia (2010). The mean plume spacing in diffusion-driven convection was observed to decrease with *Ra*.

The paper is organised as follows: we carry out experiments on natural convection due to unstable density across a semi-permeable membrane. The plume structures erupting from the thermal boundary layer are captured using PLIF visualisations. The details of experiments and flow visualisation are given in Section II. We then study the evolution of plume structures at different Ra_H and ΔC in Section II, and the special orientation of plumes and dynamics of a fully developed plume field are discussed in Section III.

II. EXPERIMENTS

The experimental setup shown in Figure 1 is fabricated to conduct convection across a semi-permeable membrane. The setup consists of a top tank and a bottom tank separated by a semi-permeable membrane. The top tank has an internal dimension of 15.6 cm × 15.6 cm with a height of 25.85 cm, contains *NaCl* solution. The bottom tank has similar inner dimensions with thicker glass walls for structural rigidity and contains NH_4Cl solution.

The semi-permeable membrane separating the top and bottom tank has a pore size of 45.6μm, a thickness of 72.5 μm and an open area factor of 0.31. The membrane is cleaned with distilled water before the experiment. The NH_4Cl solution is fed into the bottom tank from a reservoir by regulating the stop valve. The bottom tank solution is initially fed into a chamber made of a perforated acrylic plate to ensure a smooth flow of fluid into the bottom tank. The NH_4Cl solution is first allowed to rise just above the membrane, and the excess NH_4Cl solution is drained into the collecting tank using the fine control valves. This also helps to remove any trapped air bubbles, which may accumulate below the membrane and hinder the natural convection. A perpex sheet is placed on top of the membrane before pouring the *NaCl* solution into the bottom tank to avoid initial mixing before filling. The handycam and laser are then aligned properly to capture the evolution of the plume structure. The details of the flow visualisation apparatus are given in Section B. The *NaCl* solution is then carefully poured over the perpex sheet, ensuring the *NaCl* solution doesn't directly impinge on the semipermeable membrane. Convection is initiated upon removing the perpex sheet. Kinematic viscosity (ν) and mass diffusivity (D) of the top tank solution are calculated using mole fraction, using the concentration of the top tank and bottom tank solutions.

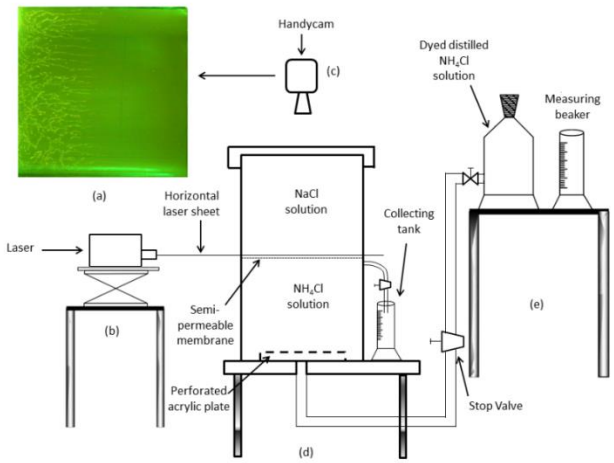

Figure 1: Schematic of experimental setup

A. Visualisation

An DPSS (Diode Pumped Solid State) Laser is used as a light source to visualise plumes erupting from the species boundary layer. The laser from the source (figure 2(a)) is converted into a diverging thin sheet using a diverging lens shown in figure 2(b). The height of the laser sheet is then carefully adjusted such that the laser sheet passes just above the semipermeable membrane, dissecting the sheet plumes erupting from the species boundary layer.

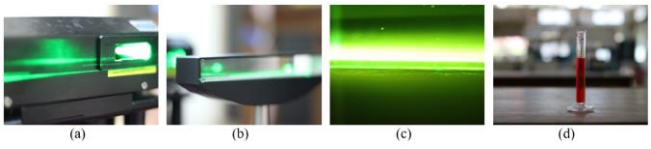

Figure 2: Flow visualisation apparatus; (a) DPSS laser, (b) diverging lens, (c) horizontal laser sheet grazing the semipermeable membrane and (d) rhodamine-6G dye

The NH_4Cl solution in the reservoir is seeded with 0.5 ppm of Rhodamine-6G at such a low concentration, the dye serves as a passive tracer, emitting bright fluorescence in contact

ISSN (Online) 2456-1290

International Journal of Engineering Research in Mechanical and Civil Engineering (IJERMCE)

Volume 12 Issue 12 December 2025

with the laser sheet. The low concentration of the dye, along with the low diffusion coefficient of Rhodamine-6G, ensures that the addition of dye doesn't introduce any measurable change in the density of NH_4Cl solution. Using this visualisation technique, plume structures erupting from the low concentration species boundary layer over the semipermeable membrane can be visualised as luminous lines in planform imaging. A DSLR camera (make SONY) is mounted vertically above the top tank, capturing the evolution of plume structures from the boundary layer as a video. These videos are then converted into frames in synch with time for qualitative analysis.

III. EVOLUTION OF PLUME STRUCTURES

The high Ra_H of the experiment ensures that the onset of evolution of plumes happens immediately after the removal of the perpex sheet to initiate convection. The evolution of plume structures was studied for 10 minutes. Three distinct stages were identified, viz, pouring dominant phase, transition phase and fully developed plume field. Higher Rayleigh number ~ 10^{11} and Schimid number ~ 600 result in a thinner species boundary layer, which results in thin sheet plumes.

A. Pouring- Dominant Phase

Plumes are initiated immediately after the initiation of convection owing to the high Ra_H of the experiments. During the initial pouring dominant phase, the dynamics of plume structures are dominated by the residual bulk flow induced during the filling of NH_4Cl in the top tank. The advective circulation across the membrane and the bulk flow in the top tank are not developed during this phase; this is evident from the lack of spatial orientation of plumes in the planform and the continuous drift of the plume-free patch. There is no consistent longitudinal motion, and the planforms are dominated by swirls and irregular billows, as shown in Figure 3. The planform of plume structure in the pouring dominant phase at different ΔC and Ra_H is shown in Figure 3.

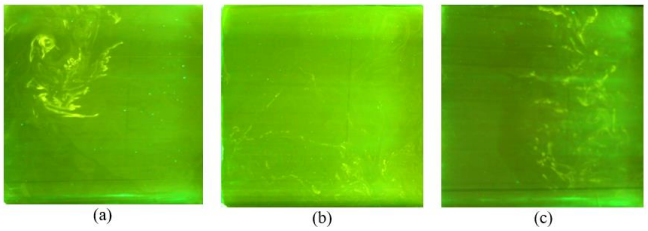

Figure 3: Planform of plume structures in pouring dominant phase; (a) Ra_H = 6.123 ×10^{10}, ΔC = 2, and Δt = 8s, (a) Ra_H = 1.845×10^{11}, ΔC = 6 and t = 14s, (c) (a) Ra_H = 2.79×10^{11}, ΔC = 9 and t = 8s.

B. Transition Phase

The transition phase is characterised by the initiation of a large number of new plumes from multiple point sources, and the lateral movement of plumes is significantly slower than the pouring dominant phase, indicating the decay of pouring-induced advection and associated shear in the top tank. During the transition phase, plumes arise from different point sources in clusters with irregular spacing and also merge with adjacent plumes.

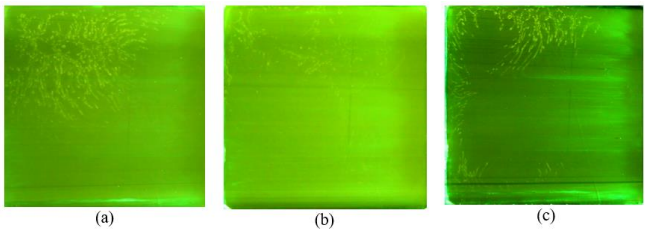

Figure 4: Planform of plume structures in pouring transition phase; (a) Ra_H = 6.123 ×10^{10}, ΔC = 2, and Δt = 53s, (a) Ra_H = 1.845×10^{11}, ΔC = 6 and t = 56s, (c) (a) Ra_H = 2.79×10^{11}, ΔC = 9, and t = 56s.

The planform of the plume structure in the transition phase at different ΔC and Ra_H is shown in Figure 4. The observed random alignment of individual plume structures in the transition phase suggests that the behaviour of plume structures in this phase is primarily governed by buoyancy-driven instabilities. This also indicates that the advective circulation across the membrane and bulk flow in the top tank are not stabilised.

C. Fully developed plume field

In a fully developed plume field, a clear horizontal orientation of plume structures with a consistent longitudinal motion is observed. In a fully developed plume field, as shown in Figure 5, the overall evolution of plumes in the planform remains stable with time. In this regime, three distinct spatial orientations were observed: (i) plume-free region, (ii) shear-aligned plume field, and (iii) instability-driven plume field. The details of these spatial regimes are discussed in Section IV. A distinct plume field indicates the existence of fully developed advective circulation across the membrane and bulk circulation in the top tank, which governs the distribution of plume structure in such convection.

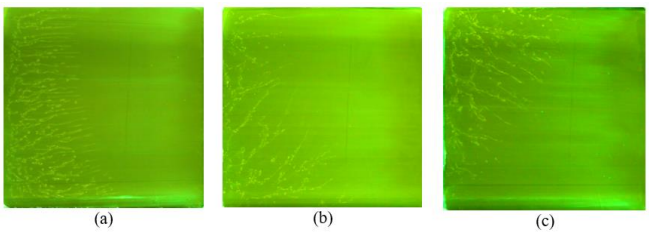

Figure 5 Planform of plume structures in fully developed plume field; (a) Ra_H = 6.123 ×10^{10}, ΔC = 2, and Δt = 10 minutes, (a) Ra_H = 1.845×10^{11}, ΔC = 6 and t = 10 minutes, (c) (a) Ra_H = 2.79×10^{11}, ΔC = 9 and t = 10 minutes.

ISSN (Online) 2456-1290

International Journal of Engineering Research in Mechanical and Civil Engineering (IJERMCE)

Volume 12 Issue 12 December 2025

IV. DYNAMICS OF THE FULLY DEVELOPED PLUME FIELD

The evolution of plume structure in a fully developed plume field doesn't spatially vary with time, indicating that both the advective circulation across the membrane and bulk circulation within the top tank have reached a coherent, fully developed state. The plume-free region (Figure 6(I)) on the right side of the planform corresponds to the downward impingement of high-concentration NH_4Cl solution, whose advective sweeping inhibits the formation of the boundary layer over the semi-permeable membrane. The advection from the bottom tank enters the species boundary layer, erupts to form plumes (II and III) and dissipates flux into the top tank. The plumes adjacent to the plume-free region are sheared by the bulk circulation existing in the top tank, resulting in an aligned plume region (II). Beyond (II), close to the wall, plumes are randomly aligned where the dynamics are purely goverened by the instability of the boundary layer.

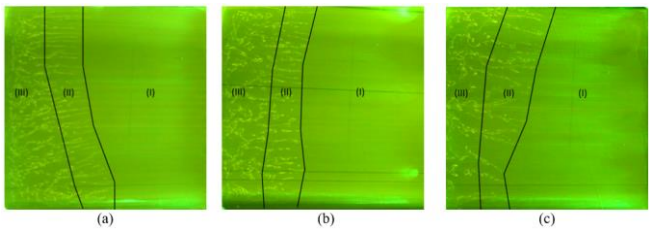

Figure 6: Spatial orientation of the fully developed plume field at different ΔC; (a) $Ra_H = 6.123 \times 10^{10}$, $\Delta C = 2$, and $\Delta t = 8$m 26s, (a) $Ra_H = 1.845 \times 10^{11}$, $\Delta C = 5$ and $t = 9$m 30s, (c) (a) $Ra_H = 2.79 \times 10^{11}$, $\Delta C = 9$, and $t = 8$m 24s. (I) represents a plume-free region, (II) aligned plume region, and (III) randomly oriented plume region.

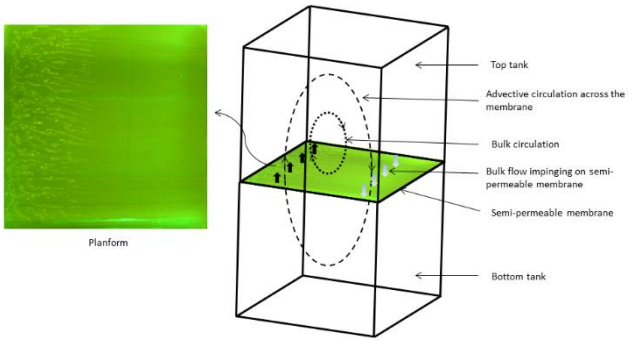

Figure 7 shows the near membrane flow dynamics in convection across a semipermeable membrane. The planform of plume structure corresponds to a $Ra_H = 6.123 \times 10^5$, $\Delta C = 2$, and $t = 6$m 30s. The dashed line represents the advective circulation across the membrane, and the dotted line represents the bulk circulation in the top tank.

The black filled arrow represents the advection from the low-concentration *NaCl* solution as rising plumes, and the gradient arrow represents the bulk flow impinging on the semi-permeable membrane. The black filled arrow represents the advection from the low-concentration *NaCl* solution as rising plumes, as shown in Figure 6(a). As the Ra_H and ΔC increase, plumes in the shear-aligned plume field become thicker and farther spaced apart. This observation is contrary to the Ra_H dependence of plume spacing in classical Rayleigh-Benard convection. This is likely due to the increase in advection into the species boundary layer, which alters the instability, thereby increasing mean plume spacing with Ra_H and ΔC.

V. CONCLUSIONS

A qualitative investigation of plume structures rising from the species boundary layer in natural convection has been studied by visualising the plumes using PLIF. The temporal evolution of plumes was observed to progress through three distinct stages: a pouring dominant phase, a transition phase and a fully developed plume field. Planforms in a fully developed plume field consist of a plume plume-free region, a shear-aligned plume field and an instability-driven plume field. Advective circulation and bulk circulation in the top tank were found to affect the dynamics of plumes erupting from the boundary layer. Plume structures were found to be much closely spaced in the shear-aligned plume field. Contrary to the conventional Ra_H dependence, mean plume spacing was found to increase with ΔC and Ra_H and mean plume thickness was found to increase with ΔC and Ra_H. These findings highlight the significant role of advective circulation and bulk circulation in modifying the plume morphology in convection across a semipermeable membrane.

REFERENCES

[1] Pera, Luciano, and Benjamin Gebhart. "Natural convection boundary layer flow over horizontal and slightly inclined surfaces." *International Journal of Heat and Mass Transfer* 16.6 (1973): 1131-1146.

[2] Mayes, C., et al. "Boundary-Layer Theory." *Physics and astronomy*. Springer Berlin Heidelberg, 2003.

[3] Gunasegarane, G. S., and Baburaj A. Puthenveettil. "Dynamics of line plumes on horizontal surfaces in turbulent convection." *Journal of Fluid Mechanics* 749 (2014): 37-78..

[4] Theerthan, S. Ananda, and Jaywant H. Arakeri. "A model for near-wall dynamics in turbulent Rayleigh–Bénard convection." *Journal of Fluid Mechanics* 373 (1998): 221-254.

[5] Puthenveettil, Baburaj A., and Jaywant H. Arakeri. "Plume structure in high-Rayleigh-number convection." *Journal of Fluid Mechanics* 542 (2005): 217-249.

[6] Puthenveettil, Baburaj A., et al. "Length of near-wall plumes in turbulent convection." *Journal of Fluid Mechanics* 685 (2011): 335-364.

[7] Shevkar, Prafulla P., et al. "On separating plumes from boundary layers in turbulent convection." *Journal of Fluid Mechanics* 941 (2022): A5.

[8] Ramareddy, G. V., et al. "Scaling in concentration-driven convection boundary layers with transpiration." *Journal of Fluid Mechanics* 903 (2020): A3.

[9] Joshy, P. J., Syam Joy, and Baburaj A. Puthenveettil. "Plume structures in natural convection with transpiration." *Journal of Flow Visualization and Image Processing* 30.3 (2023).

[10] Husar, R. B., and E. M. Sparrow. "Patterns of free convection flow adjacent to horizontal heated surfaces." *International Journal of Heat and Mass Transfer* 11.7 (1968): 1206-1208.

[11] Xia, Ke-Qing, Siu Lam, and Sheng-Qi Zhou. "Heat-flux measurement in high-Prandtl-number turbulent Rayleigh-Bénard convection." *Physical review letters* 88.6 (2002): 064501.

[12] Adrian, R. J., Rogerio TDS Ferreira, and Thomas Boberg. "Turbulent thermal convection in wide horizontal fluid layers." *Experiments in Fluids* 4.3 (1986): 121-141.

[13] Adrian, R. J., Rogerio TDS Ferreira, and Thomas Boberg. "Turbulent thermal convection in wide horizontal fluid layers." *Experiments in Fluids* 4.3 (1986): 121-141.